IEEE Access
Multidisciplinary | Rapid Review | Open Access Journal

Received June 27, 2020, accepted July 13, 2020, date of publication July 23, 2020, date of current version August 4, 2020.

Digital Object Identifier 10.1109/ACCESS.2020.3011545

ANT: Deadline-Aware Adaptive Emergency Navigation Strategy for Dynamic Hazardous Ship Evacuation With Wireless Sensor Networks

YUTING MA[1], KEZHONG LIU[1], (Member, IEEE), MOZI CHEN[1], (Graduate Student Member, IEEE), JIE MA[1], XUMING ZENG[1], KEHAO WANG[2], AND CONG LIU[3], (Member, IEEE)

[1]School of Navigation, Wuhan University of Technology, Wuhan 430000, China
[2]School of Electronics and Information Engineering, Wuhan University of Technology, Wuhan 430000, China
[3]Department of Computer Science, University of Texas at Dallas, Richardson, TX 75080, USA

Corresponding author: Mozi Chen (chenmz@whut.edu.cn)

This work was supported in part by the National Natural Science Foundation of China (NSFC) under Grant 51979216; and in part by the Major Project for the Technology Innovation of Hubei Province, China, under Grant 2017AAA120.

ABSTRACT Efficient and safe ship evacuation strategy plays a critical role in protecting passengers' lives when ships encounter accidents. Existing wireless sensor network (WSN)-based emergency navigation methods mainly consider the dynamics of hazards and accordingly plan evacuation paths to minimize human exposure to the environmental hazards, such as fire and smoke. However, without sufficient consideration of the ship capsizing time and the impact of dynamic ship inclination on the passengers' walking speed, these methods may fail to evacuate passengers before the deadline. In this paper, we propose ANT, a deadline-aware adaptive emergency navigation strategy for dynamic hazardous ship evacuation with WSNs, which informs each passenger about a hazard-avoided evacuation path to successfully reach lifeboats within the specified deadline under all circumstances. To achieve this aim, ANT analyzes the process of ship capsizing to predict the specific limited evacuation time and the worst-case traversal delay. Next, an online evacuation path planning strategy is proposed based on a real-time adaptive routing algorithm to maximize navigation efficiency while ensuring user safety. We evaluate ANT by conducting prototype experiments and extensive simulations. The results demonstrate that ANT improves the navigation success ratio by 40% and 5%, compared with state-of-the-art emergency navigation systems, namely, medial axis-based approach and ENO-based oscillation-free emergency navigation approach, respectively.

INDEX TERMS Emergency navigation, adaptive routing, ship evacuation, wireless sensor networks.

I. INTRODUCTION

Guarantee of the safety of passengers and crew of ships has received considerable attention since the International Convention for the Safety of Life at Sea was introduced by the International Maritime Organization [1]. As ship environmental hazards are dynamic and passengers are unfamiliar with the complex ship structure, accidents occurring in recent years (e.g., Costa Concordia disaster in 2012 [2]) have highlighted the chaos and catastrophic consequences of the actual ship evacuation without an intelligent location-based evacuation service [3]–[8]. Recent advances in wireless sensor networks (WSNs) have shown the potential of sensing hazards in the physical world and an in-situ interaction between people and the environment. The use of WSNs to explore dynamic environmental hazards and provide a real-time navigation service to users has garnered increasing attention.

To improve passenger safety during evacuation, significant efforts have been made to propose various WSN-assisted

The associate editor coordinating the review of this manuscript and approving it for publication was Mu Zhou.

This work is licensed under a Creative Commons Attribution 4.0 License. For more information, see https://creativecommons.org/licenses/by/4.0/

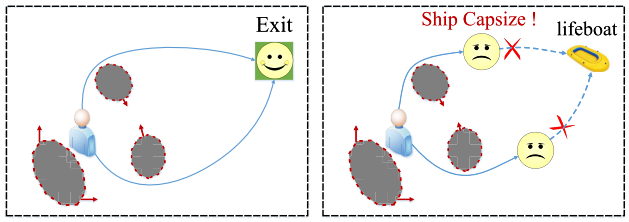

(a) Performance of OPEN in on-shore buildings (b) Performance of OPEN on ships

FIGURE 1. Performances of OPEN. The three gray regions represent dynamic hazardous regions, which are supposed to expand as indicated by the red arrows. The solid blue arrow represents the navigation path for a trapped user.

emergency navigation systems. In previous studies [9]–[14], the hazardous field has been explored using multiple sensors and safe-critical paths have been provided for users during an emergency. However, without predicting the tendency of emergency dynamics, e.g., expansion, shrinkage, and movement, the selected ''safe'' paths may be blocked by abrupt changes in hazards, thus leading to re-navigation and user oscillation. To solve this problem, follow-up studies [15]–[21] have been conducted considering the dynamics of environments and making proactive navigation decisions for users. For example, oscillation-free emergency navigation (OPEN) [15] provides navigation paths with the minimum probability of oscillation by tracking changes in hazards using a WSN and minimizing the proposed reachability-based path metric, i.e., the expected number of oscillations (ENO). These emergency navigation methods can minimize passive oscillations by making detours, thereby enhancing the path reachability in general scenarios.

However, because of the unique environmental characteristics of accidents in ships, these state-of-the-art oscillation-free emergency navigation techniques [15]–[17] cannot be directly applied on these ships. The main reason is that the ship may tilt and eventually capsize owing to water ingress after a collision or grounding [22], [23], leading to two challenges. First is that the time available for ship evacuation (i.e., the estimated time until ship capsizing, also referred to as the *deadline*) is limited. If these oscillation-free approaches provide passengers with navigation paths without oscillations but missing the deadline of ship evacuation because of large detours, it can result in catastrophic consequences. Here we take Fig. 1 as an example. To ensure that users can avoid oscillations in the dynamic hazardous ship indoor environment, the escape time provided by those approaches is likely to exceed the specified capsizing deadline. This is regarded as navigation failure. Second, the existing methods are based on the assumption that the walking speed of the users is constant; this cannot be maintained on a damaged ship. According to [24], the passengers' walking speed may significantly reduce owing to ship inclination during evacuation. Although the navigation path provided by the existing methods can ensure safe passage through the hazardous field (by estimating the available time before the hazard arrives), the user can still be delayed because of ship inclination and encounter an ever-expanding hazard. Therefore, it is vital to consider the evacuation deadline and the actual walking speed, such that passengers can successfully escape.

To address the aforementioned problems, we propose ANT, a deadline-aware adaptive emergency navigation strategy for the dynamic hazardous ship evacuation, which can provide passengers with oscillation-free navigation paths that achieve the minimum typical delay and guarantee to respect the specified deadline under all circumstances. To achieve this purpose, ANT first employs the sensing capability of sensor nodes to estimate two important deadlines: the available evacuation time before the ship sinks (overall deadline) and the arrival time of dynamic hazards (deadline of each path). Although the precise delays that will be encountered across each route during the evacuation are unknown, ANT analyzes the dynamic effect of ship inclination on the passengers' walking speed and determines the worst-case delay bound to cross each path accordingly. Based on the above-mentioned parameters, an *adaptive emergency navigation strategy*, motivated by the existing real-time scheduling theory, is proposed. In this strategy, two types of look-up tables are constructed and algorithms are developed for on-line determining routes that lead passengers to lifeboats as rapidly as possible, while guaranteeing that the worst-case traversal time does not exceed all deadlines. We evaluate ANT by conducting prototype experiments and extensive simulations. The results demonstrate that ANT improves the navigation success ratio by 40% and 5%, compared with state-of-the-art emergency navigation systems, namely, medial axis-based (MA) approach and OPEN, respectively.

The main contributions of our study are summarized as follows:

- To the best of our knowledge, this is the first ship emergency navigation solution to the dynamic deck inclination problem, and it yields predictable worst-case traversal delay times at each route and considers the ship evacuation deadline.
- Our developed on-line ship evacuation strategy, ANT, is rather light-weight, thus being practically implementable in the real world. ANT seeks to select safe paths in an adaptive way for handling the actual delays of passengers' walking, which are only revealed during run-time evacuation.
- We extensively evaluated ANT using simulations and real-world passenger ship experiments. Experimental results demonstrate that ANT outperforms state-of-the-art approaches in terms of user safety and navigation efficiency.

The remainder of this paper is organized as follows. Section II presents our motivation. The navigation model and the problem formulation are introduced in Section III. Section IV details the design of our method. We evaluate the performance of our approach through experiments on a prototype system and large-scale simulations, and these results are presented in Section V. Finally, Section VI concludes this paper.

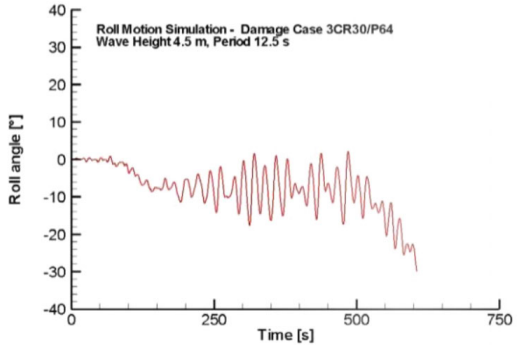

FIGURE 2. Time-history curve of the simulated ship roll motion for a specific case. Reprinted with permission from [22].

II. MOTIVATION AND PRELIMINARIES

In this section, we motivate our design by describing the unique characteristics of ship evacuation. Conventional oscillation-free navigation systems provide navigation paths by minimizing the probability of oscillation using the ENO as the path planning metric. Compared with the general environment, a damaged ship may cause two main challenges, namely, limited evacuation time and the impact on the passengers' movement speed, and make the existing methods unavailable. We now present the potential problems and insights observed from the analysis of ship accidents.

A. LIMITED EVACUATION TIME

Serious accidents at sea mainly include collisions with other ships and obstacles. According to [25], after a collision or grounding, there are risks of water ingress into the ship and sinking. In that case, the time available for ship evacuation is limited. Fig. 2 shows an example of a simulated ship roll motion behavior. We can observe that the average slope angle increases slowly at the beginning until at a certain point it starts accelerating. After a few large swings, the slope angle reaches 30° (which is regarded as the capsize criterion) and passengers' chances of survival dramatically decrease. Therefore, it is essential for the emergency navigation system to consider the limited evacuation time and navigate passengers to lifeboats before the ship capsizes. To predict the time available for ship evacuation, we consider relevant research as theoretical support. In [22], the capsizing time down to a significant wave height of 4.5 m is obtained directly using a ship motion simulation method. The method considers the loading condition of the vessel, extent and location of the damage, and sea condition in the area of operation. The probable survival time until capsizing T_c for the significant wave height lower than 4.5 m can be extrapolated with the following formula:

$$T_c = T_s \times e^{A+\frac{B}{h^2}}, \tag{1}$$

where T_s denotes the significant wave period and h indicates the significant wave height. The constants A and B can be calculated by capsizing simulations for higher wave heights using the same period T_s. In addition, considering that the presence of waves is not the only reason for ship's sinking after an accident occurs, many existing works also investigate the motion and flooding process of a damaged ship in calm water. In this paper, we refer to [26] to predict the survival time until capsizing for a ship in still water.

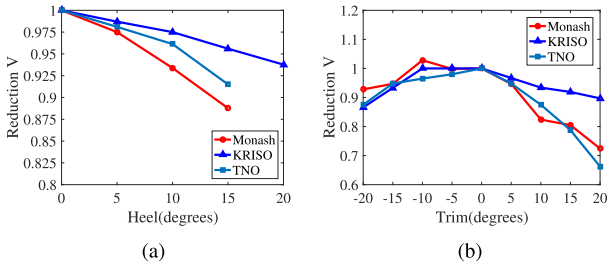

FIGURE 3. Speed reduction factor with various trim or heel angles. Fig. 3 shows the experimental results obtained from Monash [22], KRISO [24], and TNO [28].

B. IMPACT OF SHIP INCLINATION ON THE WALKING SPEED

In addition to the limited evacuation time, another challenge of ship evacuation is ship inclination. It includes heel and trim, which may significantly slow down or block the movement speed of passengers [24], [27]. Various international research projects have been concerned with the reduction in the walking speed caused by ship inclination. Fig. 3 presents speed reduction data obtained from the evacuation analyses conducted by the following organizations:

- Korea Research Institute of Ship and Ocean Engineering (KRISO)
- The Netherlands Organization for Applied Scientific Research (TNO)
- The Monash University in Australia

As can be seen, the reduction in walking speed is represented as a function of the inclination angle. When the angle reaches the maximum, the speed becomes distinctly lower than that under level conditions. According to [22], the speed reduction r_{trans} in a laterally tilted corridor can also be calculated according to the heel angle ϕ:

$$r_{trans} = \begin{cases} -0.0067\phi + 1 & 0° \le \phi < 15° \\ -0.0425\phi + 1.5375 & 15° \le \phi < 35° \\ 0.05 & 35° \le \phi \le 45° \\ 0 & 45° < \phi \end{cases} \tag{2}$$

Similarly, we can compute the speed reduction in a longitudinally tilted corridor and stairs with a lateral or longitudinal slop. Based on the above-mentioned models, we can predict the worst-case passenger traversal delay bound by observing the ship inclination degree from ship inbuilt sensors.

III. NAVIGATION MODEL AND PROBLEM FORMULATION

In this section, we first present the navigation model and then formulate the problem and provide an example to show the intuitiveness of our approach. We consider the scenario that a user equipped with a portable device has to pass through

TABLE 1. Notations and definitions of the parameters of the model.

Notation	Meaning
$\mathcal{V}$	Set of sensors
$\mathcal{E}$	Set of edges between neighboring sensors
p	Navigation path
v_h	Hazardous sensor
v_a	User sensor
v_o	Exit sensor
v_i, v_j	Two neighboring landmarks
$\overrightarrow{v_iv_j}$	Connection between v_i and v_j
$\mathcal{V}'$	Set of landmarks
$\mathcal{E}'$	Set of segments between neighboring landmarks
$\mathcal{N}_i$	Set of front neighbor landmarks of v_i
$d_T(\overrightarrow{v_iv_j})$	Typical delay along the segment $\overrightarrow{v_iv_j}$
$d_W(\overrightarrow{v_iv_j})$	Maximum delay along the segment $\overrightarrow{v_iv_j}$
$d_T(p)$	Typical delay along the path p
$d_W(p)$	Maximum delay along the path p
$D(v_j, v_i)$	Duration of hazardous arrival at $\overrightarrow{v_iv_j}$ at the initial time t_0

a field containing dynamic hazards, and the user's speed changes depending on the inclination of the ship.

A. MODEL AND DEFINITIONS

Here, we provide an in-depth description of the model and definitions, with notations presented in Table 1.

The navigation scenario on a ship is mapped to a 2-D Euclidean plane, which is well covered by a WSN. The WSN is denoted by a directed graph $G = (\mathcal{V}, \mathcal{E})$, where $\mathcal{V}$ represents the set of sensors and $\mathcal{E}$ represents the set of edges between two neighboring sensors. Evacuees on the ship are required to arrive at the place where lifeboats are located. Therefore, the sensor closest to a lifeboat is defined as *exit sensor* v_o. Other sensors are divided into two types: *hazardous sensors* and *normal sensors*, which indicate sensors inside or outside of a hazardous region, respectively. The hazardous region is modeled as a convex hull of the subset of hazardous sensors. There may be multiple hazardous regions, and because of the dynamics of hazards, the sensor status may change with time (i.e., a normal sensor may be transformed into a hazardous sensor), as shown in Figs. 4 (a)–(c). In our study, we only consider one basic type of variation in hazards, i.e., expansion.

Considering the characteristics of the indoor environment of the ship, we exploit an exit sensor and sensors at staircases as the navigation landmarks to assist the user with movement. For example, v_a, v_1, v_2, and v_o in Fig. 4d represent four different landmarks. Let $\mathcal{V}'$ be the set of landmarks, $\mathcal{V}' \subset \mathcal{V}$. The connection between two adjacent landmarks (v_i and v_j) is defined as a segment $\overrightarrow{v_iv_j}$. Let $\mathcal{E}'$ represent the set of segments, $\mathcal{E}' \subset \mathcal{E}$. In this study, we base the design of our method on the navigation model $G' = (\mathcal{V}', \mathcal{E}')$. The user is continuously guided along the segment to the next landmark until he or she reaches the exit sensor. Each segment $\overrightarrow{v_iv_j}$ in

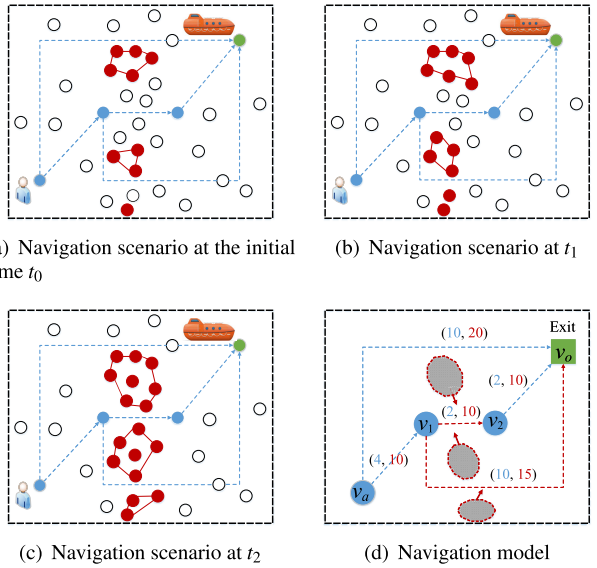

(a) Navigation scenario at the initial time t_0 (b) Navigation scenario at t_1

(c) Navigation scenario at t_2 (d) Navigation model

FIGURE 4. Navigation scenarios and the corresponding navigation model. The open circles represent normal sensors, red solid circles denote hazardous sensors, green solid circle represents an exit sensor, and blue solid circles indicate landmarks. The red dotted arrows in (d) represent the segments affected by hazards. Subgraphs (a)–(c) show the dynamics of the three hazards from t_0 to t_2.

the navigation model is labeled with two delay parameters: an estimate of the typical delay $d_T(\overrightarrow{v_iv_j})$ and a guaranteed maximum delay $d_W(\overrightarrow{v_iv_j})$ that may be encountered in traveling $\overrightarrow{v_iv_j}$ (here $0 < d_T(\overrightarrow{v_iv_j}) < d_W(\overrightarrow{v_iv_j})$). As shown in Fig. 4d, the blue number alongside each segment indicates $d_T(\overrightarrow{v_iv_j})$, and the red number denotes $d_W(\overrightarrow{v_iv_j})$.

Let $\mathcal{N}_j$ be all front neighbor landmarks of v_j in G'. $\mathcal{N}_j$ is defined as follows:

$$\mathcal{N}_j \triangleq \left\{ v_i \mid \overrightarrow{v_iv_j} \in \mathcal{E}' \right\}$$

We define $D(v_j, v_i)$, $v_i \in \mathcal{N}_j$ to reflect the duration of hazardous arrival at $\overrightarrow{v_iv_j}$ (details of the calculation procedure of $D(v_j, v_i)$ are presented in Algorithm 1). All $D(v_j, v_i)$ constitute the set $\mathcal{D}_j$. $\mathcal{D}_j$ is defined as:

$$\mathcal{D}_j \triangleq \left\{ D(v_j, v_i) \mid \overrightarrow{v_iv_j} \in \mathcal{E}' \right\}$$

Each landmark v_j in the navigation model is labeled with the set $\mathcal{D}_j$.

A navigation path p is a connected and cycle-free sequence of segments. The user sensor v_a and the exit sensor v_o are viewed as the origin and the terminal of the path, respectively:

$$p(v_a \to v_o) \triangleq \langle \overrightarrow{v_av_i}, \overrightarrow{v_iv_j}, \ldots, \overrightarrow{v_nv_o} \rangle$$

where $\overrightarrow{v_av_i} \in \mathcal{E}'$, $\overrightarrow{v_iv_j} \in \mathcal{E}'$, and $\overrightarrow{v_nv_o} \in \mathcal{E}'$. The costs $d_T(p)$ and $d_W(p)$ of path p are defined as:

$$d_T(p) \triangleq \sum_{\forall \overrightarrow{v_iv_j} \in p} d_T(\overrightarrow{v_iv_j})$$

and

$$d_W(p) \triangleq \sum_{\forall \overrightarrow{v_iv_j} \in p} d_W(\overrightarrow{v_iv_j})$$

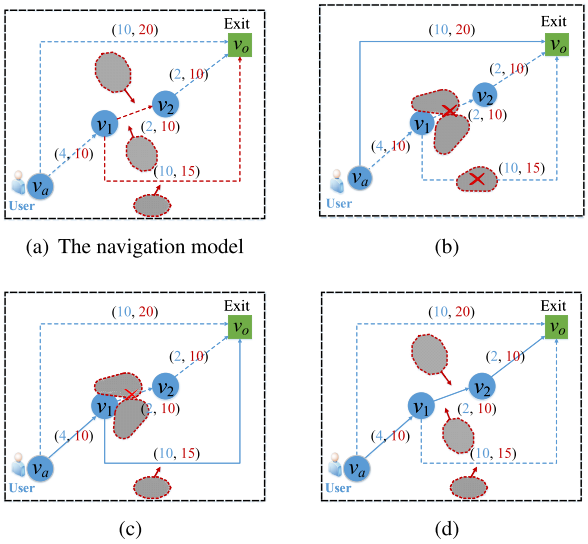

FIGURE 5. Intuitiveness of ANT. (a) Example graph of the navigation model, in which the three gray areas represent hazardous regions, red dotted arrows denote the segments affected by hazards, and blue arrows indicate all possible navigation paths. (b)–(d) Three different navigation routes that are selected based on the user's actual walking speed. The blue dotted arrows in (b)–(d) denote the paths chosen for the guided user with different velocities.

B. PROBLEM FORMULATION

Our objective is to find a *superior* path for a user who is trapped on the ship. We define a superior path to be the navigation path, p_{sup}, from the user sensor to the exit sensor with the minimum typical delay, while ensuring that the user escapes within a given deadline under all circumstances and avoids hazardous regions.

First, considering a set of segments, $\overrightarrow{v_i v_j}$, on path $p\,(v_a \rightarrow v_o)$, we present a precise definition of the superior path. Let $\mathcal{P}_i$ be all paths from v_i to v_o. We define $\mathcal{X}_i$ to represent all safe neighbors of v_i, i.e., there exists a certain path $p\,(v_i) \in \mathcal{P}_i$:

$$\mathcal{X}_i \triangleq \big\{v_j \mid d_W(\overrightarrow{v_i v_j}) + d_W(v_j \rightarrow v_y) \leq D(v_y, v_x) - d_{v_a \rightarrow v_i}, \overrightarrow{v_x v_y} \in p\,(v_i)\big\}$$

where $d_{v_a \rightarrow v_i}$ denotes the actual delay encountered from v_a to v_i, which is determined by the actual walking speed of the user.

Next, we define $\delta(v_i)$ as the minimum typical delay from v_i to exit v_o and $p_{sup}(v_i)$ as the path from v_i to v_o with $\delta(v_i)$. We have the following recurrence with respect to $\delta(v_i)$:

$$\delta(v_i) = \min_{v_j \in \mathcal{X}_i} \begin{cases} d_T(\overrightarrow{v_i v_j}) + \delta(v_j) \\ s.t.\ \ d_T(\overrightarrow{v_i v_j}) + d_W(v_j \rightarrow v_n) \leq D(v_n, v_m) \\ \quad -d_{v_a \rightarrow v_i}, \\ \overrightarrow{v_m v_n} \in p_{sup}(v_i) \end{cases}$$

Finally, a navigation path is considered to be superior if and only if for each v_i, v_j is determined by $\delta(v_i)$.

C. INTUITIVENESS OF ANT

Figs. 5 (b)–(d) provide an example to demonstrate the intuitiveness of our approach. In our scenarios, three gray areas indicate dynamic hazardous regions. The solid arrow represents the navigation path provided for the user. Subgraphs (b)–(d) show three different methods for navigating the user, depending on the user's actual walking speed. Considering the deadline C for emergency navigation on the ship, we assume $D(v_o, v_a) = D(v_o, v_2) = 27$ at the initial time; if $D(v_2, v_1) = 15$ and $D(v_o, v_1) = 20$ owing to the dynamic hazards, the selected path for the user is the solid arrow in (b). However, if $D(v_o, v_1) = 25$ and $D(v_2, v_1) = 15$, the user first traverses segment $\overrightarrow{v_a v_1}$ and then selects $\overrightarrow{v_1 v_2}$ or $\overrightarrow{v_1 v_o}$ determined by the user's actual walking speed:

1) If the actual delay, $d_{\overrightarrow{v_a v_1}}$, encountered across $\overrightarrow{v_a v_1}$ does not exceed 5, the user subsequently takes route $v_1 \rightarrow v_2 \rightarrow v_o$ (as shown in (d)) yielding a typical delay $5 + 2 + 2 = 9$, while guaranteeing that the worst-case delay to v_o is $10 + 10 \leq 27$ - $d_{\overrightarrow{v_a v_1}}$. Furthermore, the worst-case delay to v_2 is $10 \leq 15$ - $d_{\overrightarrow{v_a v_1}}$, indicating that the user can avoid the dynamic hazards in traveling from v_1 to v_2 even if the worst-case delay is 10 along this segment.

2)However, if the actual delay, $d_{\overrightarrow{v_a v_1}}$, encountered across $\overrightarrow{v_a v_1}$ exceeds 5 (but $d_{\overrightarrow{v_a v_1}} \leq 10$), the user can take route $v_1 \rightarrow v_o$ (Fig. 5c) and arrive at the exit sensor v_o within 15 (which is ≤ 27 - $d_{\overrightarrow{v_a v_1}}$). Similarly, the user avoids the dynamic hazard in moving from v_1 to v_o even in the worst-case delay of 15 along this segment ($15 \leq 25$ - $d_{\overrightarrow{v_a v_1}}$).

Thus, we can find that individual paths can be provided to users utilizing our method based on their actual walking speed. This ensures that evacuees reach the exit within the deadline while avoiding hazards.

IV. DESIGN

This section elaborates on the design of ANT. First, we present the framework of our method. Next, we provide details of ANT in the remainder of this section: quantifying the parameters of the navigation model, constructing two types of look-up tables, and guiding the movement of the user.

A. ANT FRAMEWORK

Our method is designed based on the principle of rapid routing with the guaranteed delay bound algorithm [29]. The basic process of our navigation method includes two main steps:

First, given the navigation model depicted in Fig. 4d, we establish look-up tables at each landmark during the preprocessing phase. These tables are used to determine the superior path. We construct two types of tables. One contains data in the form of a 3-tuple (s, v_j, δ), $0 < \delta < s$. The 3-tuple denotes that the path from v_i to the exit v_o, with the guaranteed worst-case delay bound s and the minimum typical delay δ, has $\overrightarrow{v_i v_j}$ as the outgoing segment from v_i. Let $\mathcal{V}''$ denote the set of landmarks affected by hazards ($v_u \in \mathcal{V}''$, if and only if there exist some segments connecting v_u with its front neighbors, which will be covered by dynamic hazards). Another table contains data in the form of a 2-tuple $(s(v_u), v_j)$, $s(v_u) > 0$, denoting that the navigation path $p\,(v_i \rightarrow v_u)$ with the guaranteed worst-case delay bound $s(v_u)$ has $\overrightarrow{v_i v_j}$ as the

outgoing segment from v_i. The second type of entry is only constructed under the following condition: if we travel $\overrightarrow{v_i v_j}$, there will be no navigation path without segments that would be damaged by dynamic hazards.

Second, the user is navigated at each intermediate landmark v_i according to the tables in the following form: first, if $C - d_{\overrightarrow{v_a v_i}} \geq s$, it is possible to take the corresponding segment $\overrightarrow{v_i v_j}$. Next, referring to another type of look-up table, if there is a remaining duration of hazardous arrival at $v_u \geq s(v_u)$, it is certain to select $\overrightarrow{v_i v_j}$.

Based on the actual walking speed of the user, our method can find a navigation path with the minimum typical delay, while enabling the user to reach the exit safely within C under all conditions. These circumstances raise two problems:

- Quantifying the parameters of the navigation model, including $d_T(\overrightarrow{v_i v_j})$ and $d_W(\overrightarrow{v_i v_j})$ on each segment $\overrightarrow{v_i v_j}$, and $\mathcal{D}_i$ attached to each landmark v_i.
- Constructing and using the two types of look-up tables to guide the user to the exit incrementally according to his actual speed.

The remainder of this section contains details of our design.

B. QUANTIFYING THE PARAMETERS OF THE NAVIGATION MODEL

This section presents the process of parameter assessment, which is the basis of constructing the look-up tables and guiding the movement of the user.

1) TYPICAL DELAY AND WORST-CASE DELAY

Ship inclination can significantly affect the movement of passengers, and consequently, the time required to traverse a certain segment also varies based on the changes in human speed. The onboard user walks at a constant speed of 0.8 m/s in rooms and corridors and 0.3 m/s on stairways [30]. Thus, we assume that the typical speed across segments is either 0.8 m/s or 0.3 m/s. In addition, we utilize the reduction factor of the walking speed when the inclination angles, including the trim and heel angles, reach 30° to assess the worst-case speed (here, this factor can be computed using Fig. 3). Let R_1 be the reduction factor for a 30° transverse to the walking direction and let R_2 be that in the walking direction. $d_W(\overrightarrow{v_i v_j})$ is computed as

$$d_W(\overrightarrow{v_i v_j}) = \frac{d_T(\overrightarrow{v_i v_j})}{R_1 \times R_2}. \tag{3}$$

2) $\mathcal{D}_j$ ON EACH LANDMARK v_j.

To evaluate $\mathcal{D}_j$ on each landmark v_j. We need to know the deadline C for emergency navigation in the dynamic hazardous ship indoor environment (here, C can be computed using (1)) and the duration of hazardous arrival at v_u.

It is necessary to traverse the segments affected by hazards before they become impassable. To predict these segments, the corresponding v_u, and the duration of hazardous arrival at v_u, we need to assess the dynamics (including the expansion direction and speed) of hazards. Fig. 6 shows the principle of determining v_u. In the figure, v_h is a hazardous

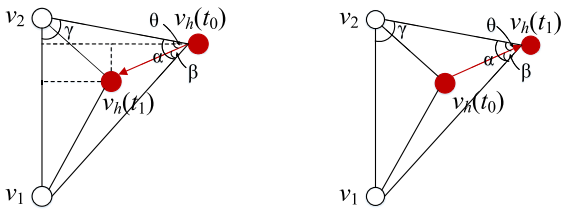

(a) v_h moves closer to a segment (b) v_h moves away from a segment

FIGURE 6. Moving tendency of the hazardous sensor v_h with a segment.

sensor, and $v_h(t_0)$ and $v_h(t_1)$ represent the locations of v_h at times t_0 and t_1, respectively. We insert v_2 into $\mathcal{V}''$ if the following conditions are satisfied. First, the hazardous node v_h is required to move closer to the segment $\overrightarrow{v_1 v_2}$ instead of departing from it. Second, $\theta \leq \alpha$ and $\beta \leq \alpha$, where θ denotes the angle between $\overline{v_h(t_0)v_2}$ and $\overline{v_h(t_0)v_h(t_1)}$, α represents the angle between $\overline{v_h(t_0)v_2}$ and $\overline{v_h(t_0)v_1}$, and β indicates the angle between $\overline{v_h(t_0)v_h(t_1)}$ and $\overline{v_h(t_0)v_1}$. The corresponding duration of hazardous arrival at v_2 is computed as follows:

$$D(v_2, v_1) = \frac{dis_{\overline{v_2 v_h(t_0)}} \times \sin\gamma}{vel_{v_h}^{\overrightarrow{v_1 v_2}}}, \tag{4}$$

where γ denotes the angle between $\overrightarrow{v_2 v_1}$ and $\overrightarrow{v_2 v_h(t_0)}$ and $dis_{\overline{v_2 v_h(t_0)}}$ indicates the distance between v_2 and $v_h(t_0)$. $vel_{v_h}^{\overrightarrow{v_1 v_2}}$ represents the velocity of v_h toward $\overrightarrow{v_1 v_2}$ (refer to [15] (Section 3.4.1) for a detailed description of the computation of $vel_{v_h}^{\overrightarrow{v_1 v_2}}$).

Next, we can compute $\mathcal{D}_j$ on each landmark v_j. We initialize all $D(v_j, v_i)$ on each landmark v_j as follows:

$$D(v_j, v_i) = \begin{cases} +\infty & \mathrm{j} \neq \mathrm{o} \\ C & \mathrm{j} = \mathrm{o} \end{cases}. \tag{5}$$

The final $\mathcal{D}_j$ at each landmark v_j is determined according to Algorithm 1.

C. CONSTRUCTING THE TWO TYPES OF LOOK-UP TABLES

We construct the two types of look-up tables to guide the user's movement. Details of the algorithm for constructing these look-up tables are provided below.

- **Look-up table to the exit:** The look-up table TAB $[v_i]$ to the exit at landmark v_i consists of 3-tuples (s, v_j, δ), with the interpretation that the path with the minimum typical delay δ from v_i to the exit v_o and the guaranteed worst-case delay bound s, has $\overrightarrow{v_i v_j}$ as the outgoing segment from v_i. The reader is referred to [29] (Section IV) for a detailed description of the LOOK-UP TABLE SYNTHESIS Algorithm to construct TAB $[v_i]$ at each landmark v_i.
- **Look-up table to $\mathcal{V}''$:** This type of entry is only constructed under the following condition: if we traverse segment $\overrightarrow{v_i v_j}$, a navigation path $p(v_i)$ without any segments that will be damaged by dynamic hazards does not exist. The pseudocode for constructing the look-up table to $\mathcal{V}''$ is shown in Algorithm 2.

Algorithm 1 Computing $\mathcal{D}_j$

Input: Dynamics of hazards; $G' = (\mathcal{V}', \mathcal{E}')$;
Output: $\mathcal{D}_j$;
Initialize $\mathcal{D}_j$ for all $v_j \in \mathcal{V}'$, as in (3) above;
for *each landmark* $v_j \in \mathcal{V}'$ **do**
  for *each landmark* $v_i \in \mathcal{N}_j$ **do**
    for *each hazardous sensor* v_h **do**
      if *the angles in* $\triangle v_i v_j v_h$ *meet the conditions in Section* IV-B **then**
        Compute $\frac{dis_{v_h}^{\overrightarrow{v_i v_j}}}{vel_{v_h}^{\overrightarrow{v_i v_j}}}$;
        if $\frac{dis_{v_h}^{\overrightarrow{v_i v_j}}}{vel_{v_h}^{\overrightarrow{v_i v_j}}} < D(v_j, v_i)$ **then**
          $D(v_j, v_i) = \frac{dis_{v_h}^{\overrightarrow{v_i v_j}}}{vel_{v_h}^{\overrightarrow{v_i v_j}}}$;
        end
      end
    end
    Insert $D(v_j, v_i)$ into $\mathcal{D}_j$;
  end
end

- **An example:** Let us now consider the process of constructing both these types of look-up tables according to the navigation model shown in Fig. 4d. First, we construct the look-up table to the exit v_o, and then we construct the look-up table to $\mathcal{V}''$ (here $\mathcal{V}''$ includes v_2 and v_o).
  1) Look-up table to the exit v_o (see Fig. 7):

D. USER NAVIGATION

We now explain how to use the final look-up tables to guide the user to the exit. We assume $C = 25$, $D(v_o, v_1) = 25$, and $D(v_2, v_1) = 20$ at the initial time. Starting from v_a, the user first traverses $\overrightarrow{v_a v_1}$ (if $20 \le C < 25$, or $C \ge 25$ but $D(v_o, v_1) < 25$ and $D(v_2, v_1) < 20$, then the user takes $\overrightarrow{v_a v_o}$). Upon reaching v_1, the user checks to determine $C - d_{\overrightarrow{v_a v_1}}$, $D(v_o, v_1) - d_{\overrightarrow{v_a v_1}}$, and $D(v_2, v_1) - d_{\overrightarrow{v_a v_1}}$:

1) If $C - d_{\overrightarrow{v_a v_1}} \ge 20$ and $D(v_2, v_1) - d_{\overrightarrow{v_a v_1}} \ge 10$, then the user traverses $\overrightarrow{v_1 v_2}$;

2) If $C - d_{\overrightarrow{v_a v_1}} \ge 20$, $D(v_2, v_1) - d_{\overrightarrow{v_a v_1}} < 10$ but $D(v_o, v_1) - d_{\overrightarrow{v_a v_1}} \ge 15$, then the user traverses $\overrightarrow{v_1 v_o}$;

3) If $15 \le C - d_{\overrightarrow{v_a v_1}} < 20$ and $D(v_o, v_1) - d_{\overrightarrow{v_a v_1}} \ge 15$, then the user traverses $\overrightarrow{v_1 v_o}$.

V. EVALUATIONS

We evaluate the developed deadline-aware adaptive emergency navigation strategy, ANT. This section presents the performance results of both experiments on real hardware and extensive simulations.

A. EXPERIMENTS ON A REAL-WORLD PASSENGER SHIP

In this part, we introduce our experiments on a real-world passenger ship, "Yangtze Gold 7." Our testbed is implemented

Algorithm 2 Constructing Look-up Table to $\mathcal{V}''$

Input: TAB $[v_i]$ on each landmark v_i; $G' = (\mathcal{V}', \mathcal{E}')$;
Output: Look-up table to $\mathcal{V}''$;
*exist*1 = FALSE // Does $p(v_i)$, which contains $\overrightarrow{v_i v_j}$, include a segment affected by hazards?;
*exist*2 = FALSE // Should the look-up table to $\mathcal{V}''$ be constructed?;
Count = 0;
for *each landmark* $v_i \in \mathcal{V}'$ **do**
  for *each* v_j *existing in* TAB $[v_i]$ **do**
    for *each* $p(v_i)$, *which contains* $\overrightarrow{v_i v_j}$, **do**
      for *each segment* $\overrightarrow{v_x v_y} \in p(v_i)$, *which contains* $\overrightarrow{v_i v_j}$, **do**
        if $\overrightarrow{v_x v_y}$ *is affected by hazards* **then**
          *exist*1 = TRUE;
        end
      end
      if *exist*1 = TRUE **then**
        Count ++;
      end
    end
    if *Count* = *the number of* $p(v_i)$, *which contains* $\overrightarrow{v_i v_j}$, **then**
      *exist*2 = TRUE;
    end
    if *exist*2 = TRUE **then**
      Call LOOK-UP TABLE SYNTHESIS Algorithm to $\mathcal{V}''$;
    end
  end
end

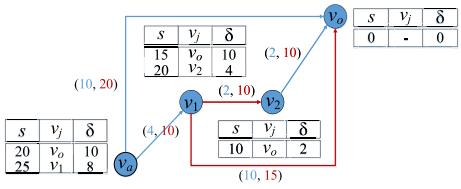

FIGURE 7. Look-up table to the exit v_o.

with Texas Instruments (TI) CC2530 chips, which meet the IEEE 802.15.4/ZigBee protocols and operate in the 2.4 GHz range. The sensor nodes are classified into *beacon nodes* and *sink nodes*. Beacon nodes are fixed inside the ship and continuously broadcast sensor messages at a rate of 1 package per second. Sink nodes collect this information from the beacon nodes and upload it to the server to determine guidance for evacuees. Through the experiments, we evaluate ANT with respect to the navigation success ratio (i.e., the number of users safely navigated to the exit within the deadline) and navigation efficiency, which is measured by the length of the route.

The experiment selected a navigation scenario that includes 25 sensors deployed into 5×5 grids with a distance

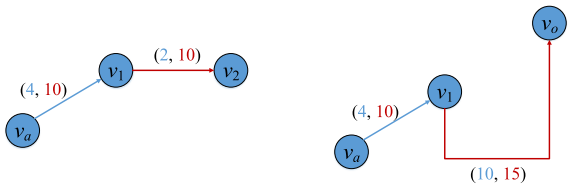

(a) Simplified model for v_2 (b) Simplified model for v_o

FIGURE 8. Simplified models for $\mathcal{V}''$.

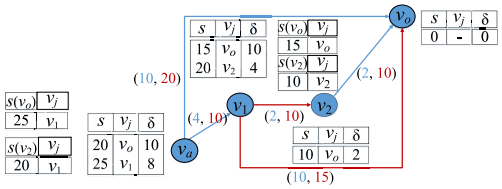

FIGURE 9. Final look-up tables.

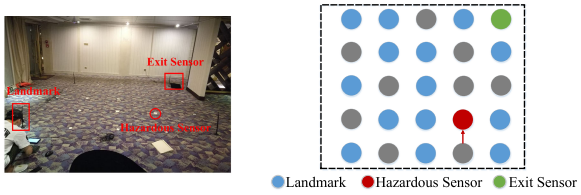

(a) (b)

FIGURE 10. Experimental setup. The hazardous region is assumed to expand as indicated by the red arrow.

of 1 m between two neighboring sensors. The sensor in the top-right corner (coordinate (5, 5)) is designated as the exit sensor, as shown in Fig. 10. We set one hazardous region consisting of one hazardous sensor because of the small-scale nature of the experiment, and the frequency and intensity of the update on hazards are utilized to represent the extent of the dynamics of hazards. Here, we select 14 sensors as the navigation landmarks based on the characteristics of the indoor environment of the ship to assist the user with movement. The typical walking speed and the worst-case speed are set to 1.2 m/s and 0.4 m/s, respectively. This allows us to compute both the typical delay and the worst-case delay for each segment based on the two speeds and the segment length. Next, we construct the two types of look-up tables at each landmark and base user navigation on these tables.

2) Look-up table to $\mathcal{V}''$ (v_2 and v_o): According to Algorithm 2, the look-up table to $\mathcal{V}''$ should be constructed on v_a and v_1, as shown in Fig. 9, based on the simplified model (illustrated in Fig. 8):

Fig. 11a depicts the escape time of our method when the human speed is set to 1.2 m/s. We see that the user always safely arrives at the exit within the deadline (the deadline is set to 23 s in our experiments). That is, the navigation success ratio of ANT reaches 100%. Fig. 11b shows the ANT efficiency in terms of path length. We can see that the path length varies with the movement speed of the user. This becomes even more significant in large-scale simulations for

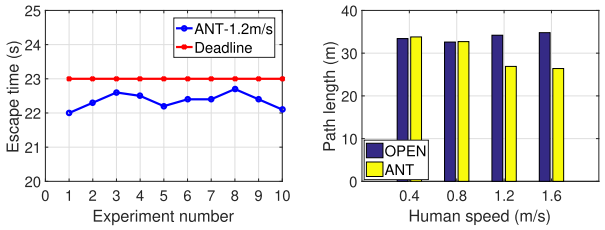

(a) (b)

FIGURE 11. (a) Escape time versus experiment number. (b) Path length versus human speed.

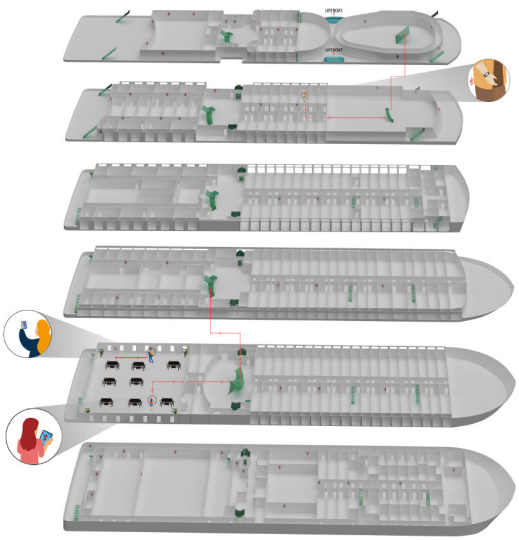

FIGURE 12. Experimental layout on a real-word passenger ship. Sensors are deployed at the locations colored red and green. We select the sensors at the green-colored locations as the landmarks.

assessing the navigation efficiency using ANT, as measured by the path length.

B. SIMULATION

In this part, we evaluate the effectiveness and scalability of ANT in a large-scale network through simulations. The performances of ANT and two state-of-the-art approaches are compared in terms of navigation efficiency and user safety perspective.

1) Simulation framework: Our simulation parameters are set using real-world passenger ship parameters. We recorded the scene parameters of the "Yangtze Gold " passenger ship, and the layout is shown in Fig. 12.

To evaluate the efficiency of ANT, we compare it with the OPEN approach [15] and MA approach [13] from four perspectives, namely, the average path length, user escape time, navigation success ratio, and minimum distance to hazardous regions. We use a network topology of a grid partitioned with 1024 to 16,384 nodes in a rectangular area. To examine the scalability, we vary the size of the network and the number of deployed nodes while retaining the same network density.

In the simulations, all users are required to arrive at the exit. We assume that hazards exhibit dynamics in only one pattern, i.e., expansion. During the simulations, we randomly insert three hazardous regions into the network and specify

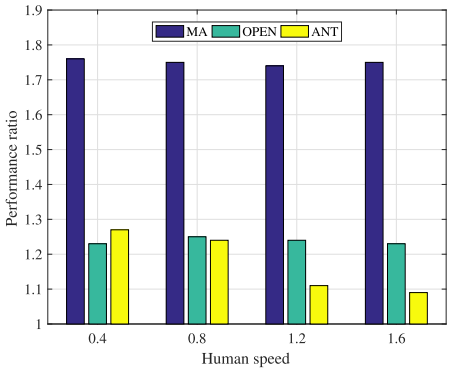

FIGURE 13. Performance ratio to the shortest path.

the dynamics of hazards as well as the walking speed of the users. The ratio of the size of each hazardous region to the total network size is maintained below 5%. Unless otherwise stated, we randomly generate 10 internal users in the field. The simulation results reported below are the average values after 20 runs.

We perform the simulation experiments written in Matlab in a personal computer (Operating System: Windows 10 Education) equipped with Intel Core i5-8400 CPU @ 2.8GHz and 8.0 GB memory. The total time needed for conducting our simulations is about 174 minutes.

2) Average length of navigation paths: We evaluate the efficiency of the path by comparing the length of the path provided by each approach L with the length of the shortest path that does not cross hazardous regions L_{OPT}. The performance ratio is defined as $\frac{L}{L_{OPT}}$. We uniformly deploy 1024 nodes in the sensor field. The worst-case speed (corresponding to the worst-case delay) and the typical speed (corresponding to the typical delay) are set to 0.4 and 1.2, respectively. Fig. 13 shows the performance ratio of the three approaches under different walking speeds. The results in the figure indicate the superior path efficiency of our method when the speed of human movement is equal to or greater than 1.2.

We further evaluate the scalability of our method in larger-scale networks. Specifically, we perform a group of simulations where the network size ranges from 2048 to 16,384, and the walking speed of the users is set to 1.2. Fig. 14a shows the performance ratio of the three approaches under different network sizes. As can be seen, MA maintains the ratio above 1.5, OPEN maintains the ratio at approximately 1.3, and our method achieves a ratio lower than 1.1. This result demonstrates that the performance ratio using our method presents distinct stability as the network size is increased. Starting from the current landmark, the user is navigated to the next superior landmark using the two types of look-up tables constructed by ANT, which means that the performance ratio does not depend on the size of the network.

We also evaluate the performance ratio by varying the number of users. We conduct a group of simulations in which the number of users is set to 20, 40, 60, 80, and 100 and the walking speed of the users is fixed at 1.2. The sensor field

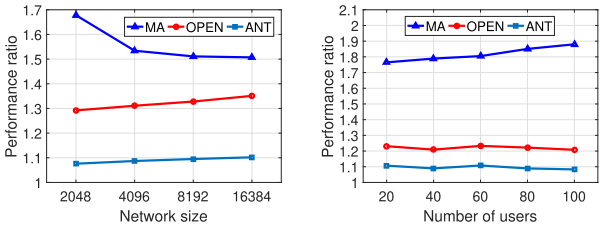

(a) Performance ratio versus network size (b) Performance ratio versus the number of users

FIGURE 14. Performance ratio to the shortest path when human speed = 1.2.

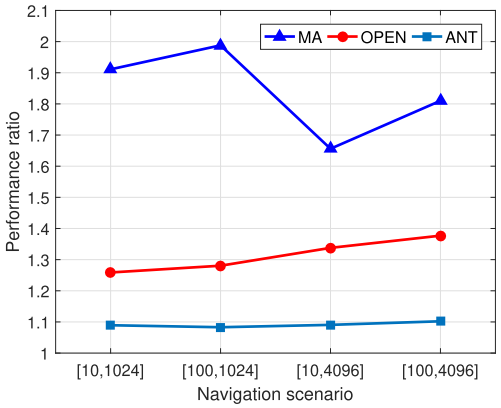

FIGURE 15. Performance ratio of the user escape time.

is uniformly partitioned with 1024 nodes. Fig. 14b shows the performance ratio to the shortest path under different numbers of users. We can see that MA has an increased ratio as the number of users is increased, whereas OPEN and our method maintain the ratio unchanged at approximately 1.2 and 1.1, respectively.

3) User escape time: The purpose of this group of simulations is to compare our method with MA and OPEN in terms of user escape time. A shorter escape time indicates a more efficient navigation path. In this simulation, 10 and 100 users are inserted into networks with sizes of 1024 and 4096, respectively. The walking speed of the users is set to 1.2. Fig. 15 shows the user escape time of the three approaches under different navigation scenarios. Our method yields a shorter escape time than the other two approaches. This is because our method can determine a safe path that avoids unnecessary detours according to the actual walking speed of the users.

4) Navigation success ratio: We evaluate the navigation success ratio of the three methods. The time available for passenger evacuation on a damaged ship is limited. Passengers must arrive at the exit before the deadline; otherwise, their navigation fails. Therefore, we can evaluate the navigation success ratio by calculating the possibility of reaching the exit within the deadline. In our simulation, this possibility is expressed as 1-$\frac{F(T)}{Q_u}$, where Q_u denotes the number of users and $F(T)$ is computed by (4).

$$F(T) = \begin{cases} 0 & T \leq C \\ T - C & T > C \end{cases}, \tag{6}$$

where T denotes the user escape time.

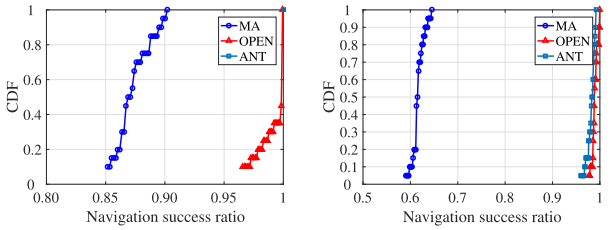

(a) Walking speed = 1.2 (b) Walking speed = 0.4

FIGURE 16. CDF of the navigation success ratio.

To compare the navigation success ratios, we consider the case in which 1024 nodes are uniformly deployed in the sensor field, and 100 users escape at the typical speed (1.2) or the worst-case speed (0.4). The deadline C is fixed at 25. Fig. 16a shows that our method outperforms OPEN and MA by always achieving a navigation success ratio of 100% when the walking speed is set to 1.2. MA and OPEN fail to ensure the navigation success in certain scenarios because they are likely to cause detours, which increases the user escape time and thus leads to the navigation failure.

Fig. 16b shows the cumulative distribution function (CDF) of the navigation success ratio of the three approaches when the speed of human movement is set to 0.4. We can see that the navigation success ratio of our method is similar to that of OPEN, where more than 96% of the users can be successfully navigated to the exit. This is because detours are inevitably included to ensure user safety when the speed of human movement is very low. Despite this, both OPEN and our method outperform MA in terms of the navigation success ratio.

Considering the influence of dynamic ship motion on the walking speed, we conduct a group of additional simulations to evaluate the navigation success ratio of the three approaches further. During the simulations, we assume that the change of the heel angle is an iterative process. Specifically, the angle increases from $-20°$ to $+20°$ and is incremented by $5°$ from segment to segment. Next, it decreases from $+20°$ to $-20°$ and is diminished by $5°$ from segment to segment. The process is repeated until users arrive at the exit node. According to the law of the change of the heel angle, we can calculate the speeds across segments (refer to the speed reduction data obtained by Monash in Fig. 3a). Here, the typical walking speed is set to 1.2, and 1024 nodes are uniformly deployed in the sensor field. The deadline C is fixed at 25. Fig. 17 shows the CDF of the navigation success ratio of the three approaches. We can see that our method outperforms OPEN and MA by achieving a nearly 100% navigation success ratio.

5) Minimum distance to hazardous regions: We evaluate the absolute safety of the path planned by the three approaches. Let B denote the minimum distance from the node on the path to hazardous regions and B_{OPT} denote the minimum distance to hazardous regions from the optimal path that maximizes B. The performance ratio is defined as $\frac{B}{B_{OPT}}$. A larger ratio indicates improved chances of the navigated user to avoid hazardous regions. Nevertheless, it is

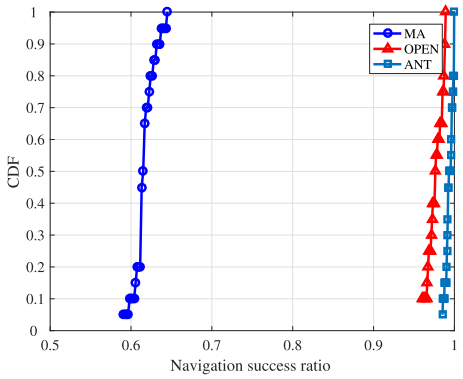

FIGURE 17. CDF of the navigation success ratio considering dynamic ship motion.

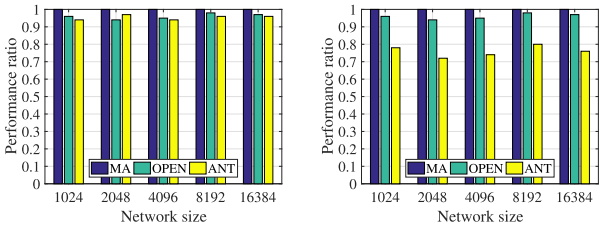

(a) Walking speed = 0.4 (b) Walking speed = 1.2

FIGURE 18. Performance ratio of the minimum distance to hazards.

unnecessary to find a path for which the maximum performance ratio is achieved because that often means that the planned path is over-conservative, which can increase the time spent in the navigation environment, thereby reducing the overall safety of the guided users.

Fig. 18a shows the performance ratio of the three approaches when the walking speed is set to 0.4. We can see that the performance ratio is not affected by the network size. The MA approach presents the optimal result with the ratio = 1. Both our method and OPEN have a performance ratio of approximately 0.95, which is slightly lower than that of MA. Fig. 18b shows the performance ratio when the speed is set to 1.2. In this case, the performance ratio of both MA and OPEN remains unchanged, whereas the ratio of our method is lower by approximately 20%, which does not indicate a considerable threat to user safety.

VI. CONCLUSION

Emergency navigation is essential for passengers (network users) on a damaged ship. Both user safety and navigation efficiency are critical requirements for successful navigation. Considering the deadline for ship evacuation and the influence of ship inclination on the walking speed, it is challenging to ensure passenger survival. In this study, based on graph theory, we design a deadline-aware adaptive emergency navigation strategy, ANT, for dynamic hazardous ship evacuation. Our method can identify a navigation path with the minimum typical delay while guaranteeing the avoidance of dynamic hazardous regions and respecting the specified deadline under all circumstances. Both small-scale experiments and extensive simulations are used to demonstrate the advantages of our method.

REFERENCES

[1] F. Stefanidis, E. Boulougouris, and D. Vassalos, "Ship evacuation and emergency response trends," in *Design and Operation of Passenger Ships*. 2019.
[2] D.-G. Yoon and C.-S. Kim, "Analysis report of the elapse for costa Concordia's disaster," *J. Korean Soc. Mar. Environ. Saf.*, vol. 18, no. 4, pp. 331–335, Aug. 2012.
[3] C. Nasso, S. Bertagna, F. Mauro, A. Marinò, and V. Bucci, "Simplified and advanced approaches for evacuation analysis of passenger ships in the early stage of design," *Brodogradnja*, vol. 70, no. 3, pp. 43–59, Sep. 2019.
[4] R. Bellas, J. Martínez, I. Rivera, R. Touza, M. Gómez, and R. Carreño, "Analysis of naval ship evacuation using stochastic simulation models and experimental data sets," *Mol. Cellular Biomechanics*, vol. 122, no. 3, pp. 971–995, 2019.
[5] M. Hu and W. Cai, "Evacuation simulation and layout optimization of cruise ship based on cellular automata," *Int. J. Comput. Appl.*, vol. 42, no. 1, pp. 36–44, Jan. 2020.
[6] J.-P. Wang, M.-R. Wang, J.-L. Zhou, Q.-J. Zuo, and X.-X. Shi, "Simulation based optimal evacuation plan in vertical ship lift: A case study," *Eng. Comput.*, vol. 37, no. 5, pp. 1757–1786, Jan. 2020.
[7] M. Chen, K. Liu, J. Ma, Y. Gu, Z. Dong, and C. Liu, "SWIM: Speed-aware WiFi-based passive indoor localization for mobile ship environment," *IEEE Trans. Mobile Comput.*, early access, Oct. 16, 2019, doi: 10.1109/TMC.2019.2947667.
[8] M. Chen, K. Liu, J. Ma, X. Zeng, Z. Dong, G. Tong, and C. Liu, "MoLoc: Unsupervised fingerprint roaming for device-free indoor localization in a mobile ship environment," *IEEE Internet Things J.*, early access, Jun. 22, 2020, doi: 10.1109/JIOT.2020.3004240.
[9] Q. Li, M. De Rosa, and D. Rus, "Distributed algorithms for guiding navigation across a sensor network," in *Proc. 9th Annu. Int. Conf. Mobile Comput. Netw. (MobiCom)*, 2003, pp. 313–325.
[10] M. Li, Y. Liu, J. Wang, and Z. Yang, "Sensor network navigation without locations," in *Proc. 28th Conf. Comput. Commun. (IEEE INFOCOM)*, Apr. 2009, pp. 2419–2427.
[11] D. Chen, C. K. Mohan, K. G. Mehrotra, and P. K. Varshney, "Distributed in-network path planning for sensor network navigation in dynamic hazardous environments," *IEEE. Trans. Wireless Commun. Mobile Comput.*, vol. 12, no. 8, pp. 739–754, Jun. 2012.
[12] G. Alankus, N. Atay, C. Lu, and O. B. Bayazit, "Adaptive embedded roadmaps for sensor networks," in *Proc. IEEE Int. Conf. Robot. Autom.*, Apr. 2007, pp. 3645–3652.
[13] J. Wang, Z. Li, M. Li, Y. Liu, and Z. Yang, "Sensor network navigation without locations," *IEEE Trans. Parallel Distrib. Syst.*, vol. 24, no. 7, pp. 1436–1446, Jul. 2013.
[14] C. Buragohain, D. Agrawal, and S. Suri, "Distributed navigation algorithms for sensor networks," in *Proc. 25th IEEE Int. Conf. Comput. Commun. (IEEE INFOCOM)*, Apr. 2006, pp. 1–10.
[15] L. Wang, Y. He, W. Liu, N. Jing, J. Wang, and Y. Liu, "On oscillation-free emergency navigation via wireless sensor networks," *IEEE Trans. Mobile Comput.*, vol. 14, no. 10, pp. 2086–2100, Oct. 2015.
[16] C. Wang, H. Lin, and H. Jiang, "CANS: Towards congestion-adaptive and small stretch emergency navigation with wireless sensor networks," *IEEE Trans. Mobile Comput.*, vol. 15, no. 5, pp. 1077–1089, May 2016.
[17] L. Wang, Y. He, Y. Liu, W. Liu, J. Wang, and N. Jing, "It is not just a matter of time: Oscillation-free emergency navigation with sensor networks," in *Proc. IEEE 33rd Real-Time Syst. Symp.*, Dec. 2012, pp. 339–348.
[18] A. A. Ahmed, M. Al-Shaboti, and A. Al-Zubairi, "An indoor emergency guidance algorithm based on wireless sensor networks," in *Proc. Int. Conf. Cloud Comput. (ICCC)*, Apr. 2015, pp. 1–5.
[19] A. Desmet and E. Gelenbe, "Reactive and proactive congestion management for emergency building evacuation," in *Proc. 38th Annu. IEEE Conf. Local Comput. Netw.*, Oct. 2013, pp. 727–730.
[20] H. Bi and E. Gelenbe, "Routing diverse evacuees with cognitive packets," in *Proc. IEEE Int. Conf. Pervas. Comput. Commun. Workshops (PERCOM WORKSHOPS)*, Mar. 2014, pp. 291–296.
[21] Z. Dong and C. Liu, "Analysis techniques for supporting hard real-time sporadic gang task systems," *Real-Time Syst.*, vol. 55, no. 3, pp. 641–666, Jul. 2019.
[22] P. Valanto, "Time-dependent survival probability of a damaged passenger ship ii-evacuation in seaway and capsizing," HSVA, Hamburg, Germany, Tech. Rep. 1661, 2006, pp. 42–62.
[23] E. Vanem and R. Skjong, "Collision and grounding of passenger ships–risk assessment and emergency evacuations," in *Proc. 3th Int. Conf. Collision Grounding Ships. (ICCGS)*, vol. 195, 2004, p. 202.
[24] D. Lee, J.-H. Park, and H. Kim, "A study on experiment of human behavior for evacuation simulation," *Ocean Eng.*, vol. 31, nos. 8–9, pp. 931–941, Jun. 2004.
[25] D. Pan, C. Lin, Z. Zhou, Y. Sun, Y. Sun, and Z. Liu, "Hydrostatic analyses of uprighting processes of a capsized and damaged ship," *Int. Shipbuilding Prog.*, vol. 65, no. 1, pp. 73–92, Jun. 2018.
[26] X. Zhang, Z. Lin, P. Li, D. Liu, Z. Li, Z. Pang, and M. Wang, "A numerical investigation on the effect of symmetric and asymmetric flooding on the damage stability of a ship," *J. Mar. Sci. Technol.*, vol. 2020, pp. 1–15, Feb. 2020.
[27] J. Sun, Y. Guo, C. Li, S. Lo, and S. Lu, "An experimental study on individual walking speed during ship evacuation with the combined effect of heeling and trim," *Ocean Eng.*, vol. 166, pp. 396–403, Oct. 2018.
[28] W. Bles, S. A. E. Nooy, and L. C. Boer, "Influence of ship listing and ship motion on walking speed," in *Proc. Int. Conf. Pedestrian Evacuation Dyn. (PED)*, 2002, pp. 437–452.
[29] S. Baruah, "Rapid routing with guaranteed delay bounds," in *Proc. IEEE Real-Time Syst. Symp. (RTSS)*, Dec. 2018, pp. 13–22.
[30] K. Yoshida, M. Murayama, and T. Itakaki, "Study on evaluation of escape route in passenger ships by evacuation simulation and full-scale trials," Res. Inst. Mar. Eng., Mitaka, Japan, Tech. Rep., 2001.

YUTING MA is currently pursuing the master's degree in marine navigation with the Wuhan University of Technology (WUT), Wuhan, China. Her research interests focus on emergency navigation and evacuation.

KEZHONG LIU (Member, IEEE) received the B.S. and M.S. degrees in marine navigation from the Wuhan University of Technology (WUT), Wuhan, China, in 1998 and 2001, respectively, and the Ph.D. degree in communication and information engineering from the Huazhong University of Science and Technology, Wuhan, in 2006. He is currently a Professor with School of Navigation, WUT. His active research interests include indoor localization technology and data mining for ship navigation.

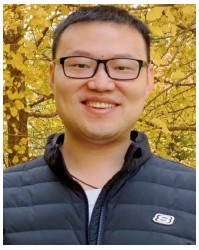

MOZI CHEN (Graduate Student Member, IEEE) received the B.S. degree in electric engineering from the Hubei University of Technology, China, in 2013, and the M.S. degree in navigation engineering from the Wuhan University of Technology (WUT), China, in 2016, where he is currently pursuing the Ph.D. degree. His research interests focus on wireless sensor networks and indoor localization.

JIE MA received the Ph.D. degree in computer science from the Huazhong University of Science and Technology, China, in 2010. He is currently an Associate Professor with the School of Navigation, Wuhan University of Technology. His researches include networked sensing systems, and data-driven intelligent transportation systems, supported by National Natural Science Foundation of China. He has over 20 published journal and conference papers in the related fields.

XUMING ZENG received the Ph.D. degree in communication engineering from the China University of Geosciences, Wuhan, China, in 2018. He is currently pursuing the Ph.D. degree in traffic and transportation engineering with the School of Navigation, Wuhan University of Technology, Wuhan, China. He has been studying wireless ad-hoc network for shipboard environment with the Wuhan University of Technology, since 2018. From 2016 to 2017, he was a joint training Ph.D. student with the Electrical and Computer Engineering, College of Engineering, Florida State University, Tallahassee, FL, USA. His research interests include routing protocols, MAC, QoS, clustering, radio resource management, traffic engineering, and performance analysis, for both wired and wireless networks.

KEHAO WANG received the B.S. degree in electrical engineering and the M.S. degree in communication and information system from the Wuhan University of Technology, Wuhan, China, in 2003 and 2006, respectively, and the Ph.D. degree from the Department of Computer Science, University of Paris-Sud XI, Orsay, France, in 2012. In 2013, he joined the School of Information Engineering, Wuhan University of Technology, where he is currently an Associate Professor. His research interests include cognitive radio networks, wireless network resource management, and embedded operating systems.

CONG LIU (Member, IEEE) received the Ph.D. degree in computer science from The University of North Carolina at Chapel Hill, in 2013. He is currently an Associate Professor with the Department of Computer Science, University of Texas at Dallas. His research interests include real-time systems and GPU. He has more than 30 published papers in premier conferences and journals. He received the Best Paper Award at the 30th IEEE RTSS and the 17th RTCSA.